Front. Phys., 2013, 8(4): 467–471
DOI 10.1007/s11467-013-0342-8

RESEARCH ARTICLE

DNA condensation and size effects of DNA condensation agent

Yan-Hui Liu[1,2,*], **Chong-Ming Jiang**[3], **Xin-Miao Guo**[1], **Yan-Lin Tang**[1], **Lin Hu**[1,†]

[1] *College of Science, Guizhou University, Guiyang 550025, China*

[2] *State Key Laboratory of Theoretical Physics, Institute of Theoretical Physics, Chinese Academy of Sciences, Beijing 100190, China*

[3] *Department of Physics, Sun Yat-Sen University, Guangzhou 510275, China*

*E-mail: *ionazati@itp.ac.cn, †lhu@gzu.edu.cn*

Received March 6, 2013; accepted April 24, 2013

Based on the model of the strong correlation of counterions condensed on DNA molecule, by tailoring interaction potential, interduplex spacing and correlation spacing between condensed counterions on DNA molecule and interduplex spacing fluctuation strength, toroidal configuration, rod-like configuration and two-hole configurations are possible. The size effects of counterion structure on the toroidal structure can be detected by this model. The autocorrelation function of the tangent vectors is found as an effective way to detect the structure of toroidal conformations and the generic pathway of the process of DNA condensation. The generic pathway of all of the configurations involves an initial nucleation loop, and the next part of the DNA chain is folded on the top of the initial nucleation loop with different manners, in agreement with the recent experimental results.

Keywords DNA condensation, Monte Carlo simulation, size effects of condensation agent

PACS numbers 87.14.Gk, 82.35.Pq, 87.15.A-, 87.15.La

1 Introduction

DNA molecule is a semi-flexible highly charged polyelectrolyte that assumes an elongated coil conformation under "physiological" conditions (a 0.1 molar solution of NaCl). Conversely, in cells millimeter-to meter-long genomic DNA is usually folded into a dense and compact state to fit within 10^{-4}–10^{-6} times smaller spaces. The remarkable compaction can be reproduced by adding a small mount of multivalent ions, such as polyamines and multivalent metal cations [1]. Both of them can induce the collapse of DNA into toroids [2–6]. Especially, the recent single molecular experiment performed using transverse magnetic tweezers [7] shows more insights into the compaction dynamics of hexamine cobalt chloride-induced DNA compaction under tension. The compaction process is discontinuous and stepwise, more sophisticated than the static structural model had suggested. During the compaction and unraveling process with constant force, distinct jumps appear. These jumps argue that turns of DNA were wrapped on the prime toroid and unwrapped from the toroids, respectively. Although much work has been done to elucidate the mechanisms of DNA condensation, until now, no consistent conclusion is drawn.

The condensation caused by multivalent ions can not be explained by the mean-field Poisson–Boltzmann theory, for the mean-field treatment of the interaction between like-charged polyelectrolyte leads inescapably to repulsive forces. To understand the origin of attractive interactions in polyelectrolyte solutions, recent theoretical work go beyond the traditional framework; two mechanisms have been suggested that led to counterion-mediated attractions. One involves a Gaussian fluctuation correction to Poisson–Boltzmann theory, first proposed by Oosawa and Manning [8, 9]. In this context of the model, Ha and Liu [10] treated the counterions as free or condensed, and the attractive interaction between two charged rods arise as a result of correlations in thermal fluctuation. The other focuses on the short-range electrostatic correlations between the counterions, and the idea of a strongly correlated two-dimension liquid of condensed counterions, similar to Wigner crystal [11], has been proposed. The mechanisms mentioned above are challenged. The Gaussian approximation, be-

ing a form of high temperature expansion, is only valid for $\xi \ll \frac{1}{\alpha^2}$, where ξ are the Manning parameter, $\xi = \frac{\beta q^2}{\varepsilon b}$, α and ε are the valence of counterions and dielectric constant of medium. However, in order to have significant counterion condensation, it is necessary to have $\xi > \frac{1}{\alpha}$. Obviously, the inequality above is violated by Gaussian approximation for multivalent counterions. The thermal fluctuation serve only to diminish the attractive interaction, and the formation of ionic crystal is not necessary [12]. In an alternative approach, Kornyshev and Leikin [13] proposed an electrostatic zipper motif that posits a helical patch for specific binding sites of polyvalent counterions on DNA. The short-range attraction responsible for condensation is a consequence of the helical structure. But recent magnetic tweezers experiment [14, 15] found that the condensation force is essentially independent of negative twist, even if the B-form DNA is transformed to an alternative structure by introducing sufficient twist.

Recently, a single experiment [16] gives a direct and significant figure about the ground state of condensed counterions, the DNA molecule in extensive phase resembles a line of negative charge with a random sequence of positive charge along its backbone, and theoretical work [17] provides more highlights on the charge distribution along DNA molecule, showing that the correlation function of the charge density displays underdamped oscillation with a characteristic length, and the amplitude of the oscillation is directly associated with the valence of the counterions, actually, which indicates that the correlation in positions of condensed counterions on DNA molecule is sufficient for DNA condensation.

Highlighted by the recent single experiment [16] and theoretical work [17], based on the correlation in positions of condensed counterions on DNA molecule, a coarse-grained but effective model is proposed to detect whether the DNA condensation depends on strong correlation of counterions and the size effects of condensation agent.

2 Model and algorithm

2.1 Theoretical model

Elasticity energy and electrostatic energy are included in the model and can be expressed as

$$E = \frac{\alpha}{2}\sum(\widehat{t}_{i+1} - \widehat{t}_i)^2 - \widetilde{N}\Delta E \qquad (1)$$

The first part in the right-hand side of Eq. (1) is responsible for the elasticity energy of DNA conformation. The DNA molecule can be modeled by N straight segments with constant length $b = 1$ nm, and $N = 200$ in our simulation. The conformation is described by the orientations of each segment $\widehat{t}_i$, i ranging from 1 to N in our simulation. The elasticity energy of every specific conformation is carried by the bending of the vertices connecting the adjacent segments $\widehat{t}_{i+1}$ and $\widehat{t}_i$, the bending energy of the vertex with unit k_BT. α is a dimensionless quantity describing the bending rigidity of the vertex,which satisfies $\alpha b = A$, and $A = 50$ nm is the persistence length of B-form DNA, thus $\alpha = 50$ in our simulation.

The attraction in DNA condensation is described as the second part in right-hand side of Eq. (1). To minimize the electrostatic energy, the condensed counterions on DNA molecule arrange themselves in a staggered configuration, called the ground state [as shown in Fig. 1(b)], which is sufficient for DNA condensation.

D, ΔE, δ and η four key parameters are included in the model, which means interduplex spacing, interduplex interaction potential, interduplex spacing fluctuation and the correlation spacing between condensed counterions, respectively. η can be identified from recent experimental and theoretical work [16–18], the all-atomic simulation [18] gives more detailed information about η, which ranges from 2–5 nm. As mentioned above, the single molecule experiment [16] provides a direct conformation of the ground state, in which there is a certain spacing between the condensed counterions. λ is the plus of the diameter of DNA molecule and the diameter of multivalent counterions. The interduplex spacing fluctuation δ is around ten percent of the interduplex spacing [19], which originates from the thermal fluctuation [20]. Due to the thermal fluctuation, the counterions will incessantly adsorb and desorb on the segments, which will cause λ to change, so D ranges from $\lambda+\delta$ to $\lambda-\delta$. Once the spacing between one positive part and one nonadjacent negative part falls in the range, the positive and negative parts are considered to be condensed, and at the same time, the total energy decrease ΔE, which mainly depends on the valence of counterions. $\widetilde{N}$ is used to index the total number of positive–negative complex.

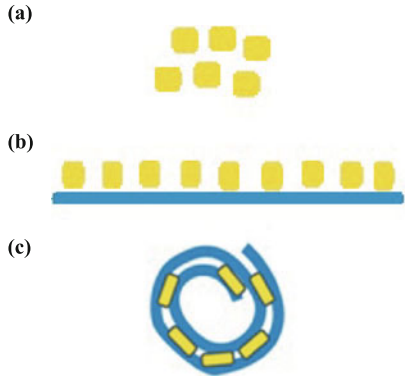

Fig. 1 Illustrations of the ground state. **(a)** The counterions. **(b)** The condensed counterions and DNA. The condensed counterions take on positive charges and the DNA between the neighbouring counterions takes on negative charges. **(c)** The condensed phase.

2.2 Algorithm

As for the algorithm, the Metropolis–Monte Carlo procedure [21] is used for the statistical sampling of chain conformations. During the simulation process, two steps of perturbation moves were used, and both steps are global. For step (I), two non-neighboring vertices were randomly selected in the DNA chain, and the part between the two selected vertices rotated around the axis, which pass through the two selected vertices. The rotation angle applied for the move is uniformly distributed in the range of $[0, \phi]$, where ϕ is the upper bound determined by the acceptance ratio. After the vertices mentioned in step (I) are selected, a rotation of the left (right) part of the chain with respect to a random axis that passes through the selected vertex is applied. The orientation of the axis is uniformly distributed in space, and the rotation angle applied for the move is also uniformly distributed in the range of $[0, \phi]$, where ϕ is the upper bound determined by the acceptance ratio. The probability of accepting a trial conformation is obtained by applying the standard Metropolis rules.

3 Results and discussion

3.1 Autocorrelation of tangent vectors and effects of interduplex spacing fluctuation δ and interduplex spacing

For a long linear DNA molecule, its autocorrelation of tangent vectors [22] can be expressed as

$$\langle \hat{t}(s) \cdot \hat{t}'(s) \rangle = \exp\left(\frac{-|s - s'|}{l_p}\right) \tag{2}$$

l_p is the persistence length of DNA molecule. Therefore, the autocorrelation of tangent vectors falls off exponentially with contour distance along DNA molecule. Randomly choose a position s on circular DNA as reference point, with the separation between reference point s and position s' increasing, and the autocorrelation of tangent vectors decreases from 1 to the minimum, while $s - s'$ equals to half of contour length of circular DNA. Moving ahead along circular DNA molecule, the $s - s'$ decreases from half of contour length to zero, so that the autocorrelation of tangent vectors increases from the minimum to 1. If more than one regular circular structure appears in the condensation states of linear DNA molecule, one can expect that the autocorrelation of tangent vectors as a function of s will oscillate periodically, just like cosine function, and every period represents one circular structure as the uppers in Fig. 2 and Fig. 3). Interduplex spacing fluctuation and interduplex spacing have effects on the condensed conformations. Their changing makes the conformations plentiful, such as rod-like conformations and two-hole conformations, and the periodical autocorrelation of tangent vectors corresponds to the condensed toroidal structure (as the lowers shown in Fig. 2 and Fig. 3).

One common feature can be justified from the autocorrelation of tangent vectors in Fig. 2 and Fig. 3, namely, the generic pathway of all of the configurations involves an initial nucleation loop, and the next part of the DNA chain is folded on the initial nucleation loop with different manners. This is consistent with recent experimental results that the condensation process initiates with a loop structure [14, 15].

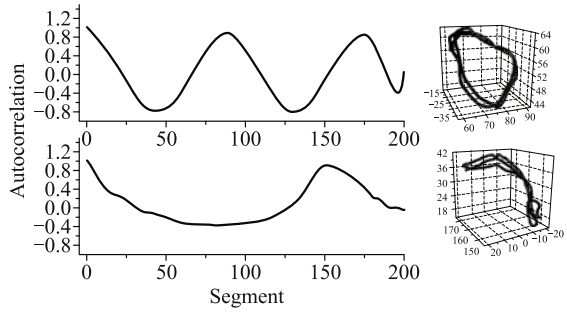

Fig. 2 Effects of interduplex spacing D. All autocorrelation and conformations have the same interduplex energy ($\Delta E = -6k_BT$), interduplex spacing fluctuation ($\delta = 0.2$ nm) and the correlation spacing between condensed counterions ($\eta = 2.0$ nm), but with different interduplex spacing (D), from up to down, 2.2 nm and 2.6 nm, respectively.

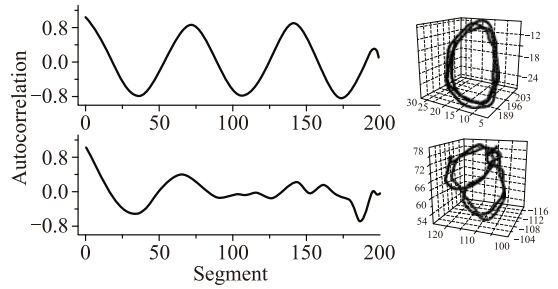

Fig. 3 Effects of interduplex spacing fluctuation (δ). All autocorrelation and conformations have the same interduplex energy ($\Delta E = -15k_BT$), the plus of the diameter of DNA molecule and the diameter of multivalent counterion $\lambda = 2.0$ nm, and the correlation distance between condensed counterions ($\eta = 2.0$ nm), but with different interduplex spacing fluctuation (δ), from up to down, 0.2 nm and 0.1 nm, respectively.

3.2 Effects of the condensation agent structure

In the simulation work, the correlation spacing between condensed counterions η equals to 2 nm, the parameter ΔE ranges from $-6k_BT$ to $-15k_BT$. According to the parameter λ, all the results can be outlined into column I and column II, with $\lambda = 2.0$ nm and $\lambda = 2.2$ nm, repectively (as shown in Fig. 4). For the column II, except the

point with $\Delta E = -7k_BT$ (its interduplex spacing fluctuation δ is 0.2 nm), the interduplex spacing fluctuation δ for all the other points is 0.1 nm, so the interduplex spacing D ranges from 2.0 nm to 2.4 nm, For the column I, $\delta = 0.1$ nm, so the interduplex D falls into [1.8 nm, 2.2 nm]. Both are reasonably consistent with the all-atomic simulation results [18] and experimental results [23, 24]. while the hexamine cobalt (III) is used as condensation agent, the interduplex spacing is about 2.7nm center to center [23] and the interduplex spacing for DNA in viral capsid and in crystals is about 2.67 nm [24].

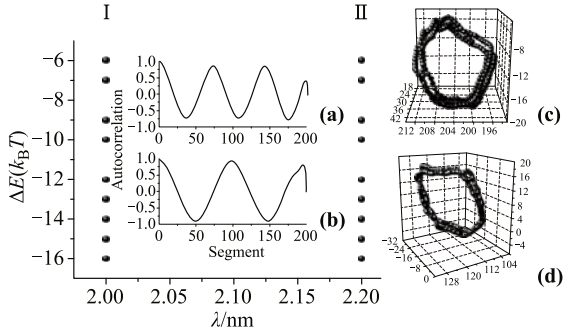

Fig. 4 Phase diagram of DNA condensation. The interaction potential ranges from $-6k_BT$ to $-16k_BT$. The parameter λ corresponding to column I and II is 2.0 nm and 2.2 nm, respectively. Every filled point in the phase diagram represents toroidal conformation. **(c)** (in column I) and **(d)** (in column II) are the toroidal conformation with the same interaction potential $-12k_BT$, but with different λ. **(a)** and **(b)** are the autocorrelation of tangent vectors corresponding to (c) and (d), respectively.

In Fig. 4, the case with interaction potential $\Delta E = -12k_BT$ is taken as an example, Fig. 4(a) and (c) represent the autocorrelation and conformation of the point with interaction potential $\Delta E = -12k_BT$ in column I, and Fig. 4(b) and (d) represent the autocorrelation and conformation of the point with interaction potential $\Delta E = -12k_BT$ in column II. Judging from the autocorrelation, the conformation c contains three loops and the conformation d contains two loops. Obviously, the DNA molecule at points in column I is folded more compactly than the one at points in column II, indicating that its radius of conformation at points in column I is smaller than the corresponding one in column II.

The two points taken as example have the same interduplex interaction potential, interduplex spacing fluctuation and the correlation spacing between condensed counterions, respectively, so the differences between their conformations and autocorrelations are caused by the interduplex distance. Actually, the essence of this phenomenon originates from the effects of counterion structure. Experiments [25–27] have pointed out that hexamine cobalt (III) is an isovalent analogue of spermidine and a trivalent cation with spherical symmetry in contrast to the elongated spermidine with its charge separated by methylene bridges, and concluded that the morphology of condensates and the size distribution of toroids depend on the counterion structure. The radius of toroidal structures condensed by hexamine cobalt (III) is smaller than the one by spermidine. These experiment results are totally consistent with the corresponding points in column I and II, which should represent the condensation caused by the counterions with the same interaction potential (same valence) but with different structure, namely, with different λ.

4 Conclusions and perspective

The simulation results from our model provided abundant condensation conformations, such as toroidal structure, rod-like structures and two-hole toroidal structures (as shown in Fig. 2), all of which have been found in the experimental results before [28, 29], suggesting that the ground state can produce the attraction in the condensation process. By using the autocorrelation function of the tangent vectors, the structure of toroidal conformations can be detected effectively and it is found that the generic pathway of all of the configurations involves an initial nucleation loop and the next part of the DNA chain is folded on the top of the initial nucleation loop with different manners. At last, the size effects of counterion structure on the toroidal structure can be detected by this model.

The bending rigidity, even for the nonlinear elastic condition, is an important factor in DNA condensation. Especially, experimental results show that ion concentration and temperature can alter the DNA molecule bending rigidity [30, 31], and how the bending stiffness affect the DNA condensation should be investigated urgently. The autocorrelation of tangent vectors tells how much loop has wrapped on the condensates nucleate. So the coarse-grain model have potential to detect effects of bending rigidity on the DNA condensation quantitatively. This model can also be employed to investigate the magnetic tweezers experiment with force applied on DNA molecule.

Acknowledgements This work was supported by the National Natural Science Foundation of China under Grant Nos. 11047022 and 11204045, Guizhou Provincial Tracking Key Program of Social Development under Grant Nos. SZ20113069 and SY20123089, the Research Foundation from Ministry of Education of China (Grant No. 2012152), and the Grant for Visiting Scholar of the Key Laboratory of Biorheological Science and Technology of Ministry of Education (Chongqing University).

References

1. N. V. Hud and I. D. Vilfan, Toroidal DNA condensates: Un-

raveling the fine structure and the role of nucleation in determining size, *Annu. Rev. Biophys. Biomol. Struct.*, 2005, 34: 295

2. V. A. Bloomfield, DNA condensation,*Curr. Opin. Struct. Biol.*, 1996, 6(3): 334
3. A. Leforestier, A. Siber, F. Livolant, and R. Podgornik, Protein-DNA interactions determine the shapes of DNA toroids condensed in virus capsids, *Biophys. J.*, 2011, 100: 2209
4. Z. Y. Ou and M. Muthukumar, Langevin dynamics of semiflexible polyelectrolytes: Rod-toroid-globule-coil structures and counterion distribution, *J. Chem. Phys.*, 2005, 123(7): 074905
5. W. M. Gelbart, R. F. Bruinsma, P. A. Pincus, V. A. Parsegian, and W. J. Johnson, DNA-inspired electrostatics, *Phys. Today*, 2000, 53: 38
6. B. Schnurr, F. C. MacKintosh, and D. R. M. Williams, Dynamical intermediates in the collapse of semiflexible polymers in poor solvents, *Europhys. Lett.*, 2000, 51: 279
7. W. B. Fu, X. L. Wang, X. H. Zhang, S. Y. Ran, J. Yan, and M. Li, Compaction dynamics of single DNA molecules under tension, *J. Am. Chem. Soc.*, 2006, 128(47): 15040
8. F. Oosawa, Interaction between parallel rodlike macroions, *Biopolymers*, 1968, 6(11): 1633
9. G. S. Manning, Limiting laws and counterion condensation in polyelectrolyte solutions (i): Colligative properties, *J. Chem. Phys.*, 1969, 51(3): 924
10. B. Y. Ha and A. J. Liu, Counterion-mediated attraction between two like-charged rods, *Phys. Rev. Lett.*, 1997, 79(7): 1289
11. I. Rouzina and V. A. Bloomfield, Macroion attraction due to electrostatic correlation between screening counterions (1): Mobile surface-adsorbed ions and diffuse ion cloud, *J. Phys. Chem.*, 1996, 100(23): 9977
12. Y. Levin, J. J. Arenzon, and J. F. Stilck, The nature of attraction between like-charged rods, *Phys. Rev. Lett.*, 1999, 83(13): 2680
13. A. A. Kornyshev and S. Leikin, Electrostatic zipper motif for DNA aggregation, *Phys. Rev. Lett.*, 1999, 82(20): 4138
14. K. Besteman, S. Hage, N. H. Dekker, and S. G. Lemay, Role of tension and twist in single-molecule DNA condensation, *Phys. Rev. Lett.*, 2007, 98(5): 058103
15. K. Besteman, K. Van Eijk, and S. G. Lemay, Charge inversion accompanies DNA condensation by multivalent ions, *Nat. Phys.*, 2007, 3(9): 641
16. F. Ritort, S. Mihardja, S. B. Smith, and C. Bustamante, Condensation transition in DNA-polyaminoamide dendrimer fibers studied using optical tweezers, *Phys. Rev. Lett.*, 2006, 96(11): 118301
17. W. K. Kim and W. Sung, Charge density coordination and dynamics in a rodlike polyelectrolyte, *Phys. Rev. E*, 2008, 78(2): 021904
18. L. Dai, Y. G. Mu, L. Nordenskiöld, and J. R. van der Maarel, Molecular dynamics simulation of multivalent-ion mediated attraction between DNA molecules, *Phys. Rev. Lett.*, 2008, 100(11): 118301
19. F. Oosawa, Polyelectrolyte, New York: Marcel Dekker, INC, 1971
20. J. Barrat and J. Hansen, Basic Concepts for Simple and Complex Liquids, Cambridge: Cambridge University Press, 2003
21. Y. H. Liu and L. Hu, Monte Carlo simulation on topology of DNA minicircles, *Chinese J. Comput. Phys.*, 2009, 26: 152 (in Chinese)
22. J. Marko, Introduction to single-DNA micromechanics in multiple aspects of DNA and RNA from biophysics to bioinformatics Les Houches Session LXXXII, Elsevier, 2005
23. L. S. Lerman, L. S. Wilkerson, J. H. Venable, Jr, and B. H. Robinson, DNA packing in single crystals inferred from freeze-fracture-etch replicas, *J. Mol. Biol.*, 1976, 108(2): 271
24. J. A. Schellman and N. Parthasarathy, X-ray diffraction studies on cation-collapsed DNA, *J. Mol. Biol.*, 1984, 175: 313
25. H. Deng and V. A. Bloomfield, Structural effects of cobalt-amine compounds on DNA condensation, *Biophys. J.*, 1999, 77(3): 1556
26. G. E. Plum, P. G. Arscott, and V. A. Bloomfield, Condensation of DNA by trivalent cations (2): Effects of cation structure, *Biopolymers*, 1990, 30(5–6): 631
27. J. Widom and R. L. Baldwin, Monomolecular condensation of lambda-DNA induced by cobalt hexamine, *Biopolymers*, 1983, 22(6): 1595
28. J. A. Benbasat, Condensation of bacteriophage phi W14 DNA of varying charge densities by trivalent counterions, *Biochemistry*, 1984, 23(16): 3609
29. A. M. Carnerup, M. L. Ainalem, V. Alfredsson, and T. Nylander, Watching DNA condensation induced by poly (amido amine) dendrimer with time-resolved cryo-TEM, *Langmuir*, 2009, 25(21): 12466
30. G. S. Manning, The persistence length of DNA is reached from the persistence length of its null isomer through an internal electrostatic stretching force, *Biophys. J.*, 2006, 91(10): 3607
31. S. Geggier, A. Kotlyar, and A. Vologodskii, Temperature dependence of DNA persistence length, *Nucleic Acids Res.*, 2011, 39(4): 1427